Digital-Physical Hybrid Simulation for Demand Response Analysis of Copper Electrorefining Processes

Yuze Zhao, Zhaonan Zhang, Xiandong Xu
Yide Han, Xiaodan Yu, Hongjie Jia
State Key Laboratory of Smart Power Distribution Equipment and System, Tianjin University
Tianjin, China

Lidong Zhang, Changpeng Song
School of Energy and Power Engineering
Northeast Electric Power University
Jilin, China
Correspondence: yuzezhao@tju.edu.cn

***Abstract*—Global copper demand has rapidly increased due to renewable energy and electric vehicle development. The copper electrorefining process, which consumes 300-400 kWh/t, has high demand response (DR) capacity. However, existing experimental and simulation approaches, which are more based on reaction mechanism elucidation, are inadequate for real-time analysis of the impact of DR on production. A Digital-Physical Hybrid Simulation method is proposed to address the limitations of purely digital or physical simulations. A simplified electrolysis model is coupled with a scaled physical cell that periodically corrects digital parameters, achieving synchronized co-simulation. The system monitors cell voltage and copper yield to evaluate energy consumption and production capacity during DR. Experimental validation shows voltage prediction errors less than 1.5% and cathode yield errors under 1.3%, confirming the method′s accuracy and feasibility.**

***Index Terms*--copper electrolysis, digital modeling, hybrid simulation, physical model.**

I. INTRODUCTION

Global copper demand has markedly increased with the expansion of renewable energy and electric vehicle (EV) industries, where EVs consume nearly three times more copper than conventional vehicles [1]. According to the International Energy Agency, low-carbon technologies will account for about 40% of global copper demand by 2040 [2], and overall demand is projected to triple between 2010 and 2050 [3]. High-purity copper (>99.99%) is mainly produced via electrolytic refining, an energy-intensive process requiring 300–400 kWh per ton.

About 70% of refined copper is used in electrical and telecommunication applications [4]. To obtain these copper, both pyrometallurgical and hydrometallurgical processes must undergo electrolytic refining-an exceptionally energy-intensive procedure [3]. In the electrolytic process, optimize operational scheduling can reduce annual electricity costs in copper electrolysis by up to 14.2%, revealing substantial potential for demand response (DR) applications [3].

However, in practical industrial operation, the copper electrolysis process generally maintains a highly stable operating condition, such as electrolyte temperature control around 65 °C [5]. Participation in DR inherently perturbs this stability, as load adjustments alter the electrolysis cell's operating state, such as altering the current according to the DR instructions will affect the cell temperature, which in turn will influence the deposition process of the cathode copper and cell voltage. Furthermore, frequent DR participation may disrupt production continuity, prolong the electrolytic cycle, and necessitate coordinated adjustments in preceding pyrometallurgical stages. Therefore, the development of a computational decision-support model to assist operators in process control and hazard prediction during DR participation is both necessary and valuable.

Existing models primarily adopt multiphysics coupling [6] and reaction kinetics–based approaches [7] for simulation. Computational fluid dynamics was employed by Kawai et al. to simulate industrial-scale flow behavior, effectively capturing multiphase dynamics [8]. Conductivity and viscosity models for industrial electrolytes were validated by Ashrafi-Nasrabadi et al., with impurity effects being incorporated [9]. Although these studies provide valuable insight into the electrolysis process, their high computational demand leads to prolonged solution times, rendering them unsuitable for real-time or multiscenario simulation in industrial workshop environments.

However, pure physical simulation cannot fully monitor real-time operating variables of the equipment. For instance, the cathode copper yield can only be obtained by weighing after the experiment, and the composition of highly concentrated electrolytes cannot be analyzed online.

To address this limitation, a hybrid modeling approach may be adopted to enable real-time, scaled-down, process correlation simulation capability, the main contributions are:

1) Develop a simplified digital model that captures the dynamic behavior of electrolytic process and outputs the primary operational indicators of interest to plant operators, such as cell voltage, production yield, and electrolyte level.

2) Establish a digital-physical hybrid simulation platform and its information interaction mechanism can support electrolytic workshops in participating in DR programs.

3) High-precision real-time simulation was achieved through the synchronized operation of the digital and physical systems. This result demonstrates the technical advantages of the proposed approach in real-time simulation applications.

The authors gratefully acknowledge the support of National Key R&D Program of China (2023YFB2407300) and National Natural Science Foundation of China (52577133).

II. Modeling of Digital-Physical Hybrid Model

A. The Principle of Copper Electrolytic Refining

Copper electrorefining is an electrolytic purification process in which impure copper (anode) and pure copper or stainless steel (cathode) are immersed in an electrolyte composed of copper sulfate and sulfuric acid. When an electric current is applied, copper at the anode dissolves into the electrolyte as Cu^{2+} ions, while impurities are separated. The copper ions are subsequently reduced and deposited onto the cathode, as illustrated in Fig. 1.

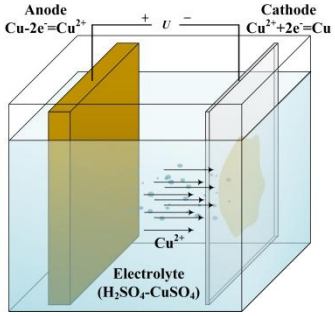

Figure 1. The principle of copper electrolytic refining.

When electrolysis cells participating in DR, energy consumption is primarily regulated by adjusting the steam heating of the electrolyte, the cell current, and the pump frequency. Therefore, in developing the digital model, particular emphasis should be placed on the coupled energy (temperature) and mass variations within the cell. In the smart controller of the physical model, the electrolysis process is likewise controlled by adjusting the aforementioned variables.

During the production of electrolytic copper, the principles of energy conservation and mass conservation must inherently be satisfied. Within the electrolytic system, there exist continuous inflows and outflows of both matter and energy. Among all components, the electrolyte is regarded as the core element of the system, for the following reasons:

1) The electrolyte serves as the intermediate medium for copper ion transport from the anode to the cathode.

2) The temperature, composition, and circulation rate of the electrolyte directly influence the quality and yield of cathode copper.

B. Digital model

In the development of the digital model of operating status, the electrolyte-centered framework is adopted to compute and iteratively track the temporal evolution of energy and material exchanges within the system. By calculating the parameters such as cell temperature and conductivity within a time step, the dynamic analysis of the operation status of the electrolytic cell can be achieved. Furthermore, during the construction of the digital model, it is essential to differentiate between continuous and event-driven processes in the electrolysis operation. The variations of energy and material flows within the electrolytic cell are illustrated in Fig. 2.

The energy variation within the electrolyte over a single time step is as follows:

$$\Delta\Theta_{\mathrm{ele,t}} = W_{\mathrm{cont}} + W_{\mathrm{event}} \tag{1}$$

$$\partial W_{\mathrm{cont}}/\partial t = P_{\mathrm{heat}} + P_{\mathrm{pum}} + P_{\mathrm{ele}} - P_{\mathrm{heat}}^{\mathrm{loss}} \tag{2}$$

$$W_{\mathrm{event}} = E_{\mathrm{ano}} + E_{\mathrm{cath}} + E_{\mathrm{new}} - \delta_{\mathrm{ano}} - \delta_{\mathrm{cath}} - \delta_{\mathrm{mud}} \tag{3}$$

where W_{cont} and W_{event} denote the energy inputs from continuous and event-driven processes, respectively. Meanwhile, the triggering of W_{event} is often accompanied by intermittently periodic changes, such as electrode replacement and electrolyte replenishment insertion; these variations may also be categorized as event-driven processes. P_{heat}, P_{pum} and P_{ele} are corresponds to the electrolyte heating energy, pump power input, and Joule heat generated by the current, respectively. $P_{\mathrm{heat}}^{\mathrm{loss}}$ represents the heat loss to the environment. E_{ano} and E_{cath} denotes the temperature perturbation caused by anode and cathode insertion, respectively. E_{new} represents the temperature change due to electrolyte make-up. δ_{ano}, δ_{cath} and δ_{mud} denote the temperature perturbations caused by anode, cathode and anode mud removal.

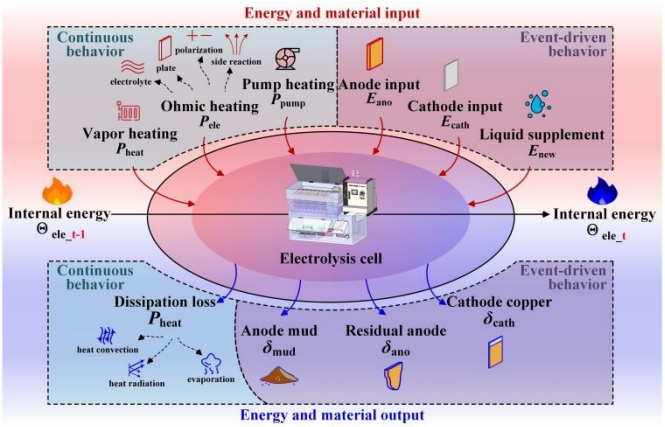

Figure 2. Energy-mateiral flow within the electrolytic cell.

1) Continuous Behavior

The continuous behavior mainly include electrolyte heating by steam, the circulation pump, and electrolysis current, as well as heat dissipation losses. So the continuous behavior is characterized by differentiable, power-type inputs. The corresponding calculations are given as follows.

a) Steam and pump power heating

Steam heating (P_{heat}) constitutes the primary energy input for maintaining the cell temperature, and its magnitude is determined by the heat exchanger efficiency and the heat transfer rate; their product yields the steam-heating power. Meanwhile, to enable recirculative heating of the electrolyte, additional energy is introduced through the circulation pump (P_{pum}), which is given by the product of the pump power and the pump efficiency.

b) Electrolytic current heating

During the electrolysis process, the heat generated by the electrolytic current primarily consists of three components: ohmic heating of the electrolyte, ohmic heating of the cathode plate, and heat generation resulting from polarization losses at both the anode and cathode. The electrolytic current heating (P_{ele}), can be expressed as follows:

$$P_{\text{ele}} = P_{\text{ele,heat}} + P_{\text{cath}} + P_{\text{pol}} \quad (4)$$

where $P_{\text{ele,heat}}$ and P_{cath} are the ohmic heating power of the electrolyte and cathode, respectively. P_{pol} is the heating power generated by polarization effects at the plates.

(i) Ohmic heating

Ohmic heating in both the electrolyte and the electrodes can be determined using Ohm's law as follows:

$$P_{\text{ele,heat}} = I^2 \bullet R_{\text{ele}} \quad (5)$$

$$P_{\text{cath}} = I^2 \bullet R_{\text{cath}} \quad (6)$$

where I is the cell current, R_{ele} and R_{cath} denotes the electrical resistance of the electrolyte and the electrode plates, respectively.

(ii) Polarization heating

The heat generated by electrode polarization can be calculated as:

$$P_{\text{pol}} = I \cdot (\eta_{\text{and}} + \eta_{\text{cath}}) \quad (7)$$

where P_{pol} denotes the polarization heat generation. η_{and} and η_{cath} are the anodic and cathodic overpotentials.

c) Heat dissipation losses

During the copper electrorefining process, heat dissipation primarily occurs through the following mechanisms:

$$P_{\text{heat}}^{\text{loss}} = P_{\text{conv}} + P_{\text{radi}} + P_{\text{evap}} \quad (8)$$

where $P_{\text{heat}}^{\text{loss}}$ denotes the total heat loss. P_{conv}, P_{radi}, and P_{evap} represent the three heat-loss pathways, i.e., convective heat transfer, radiative heat transfer, and evaporative heat loss from the electrolyte surface in open-type electrolytic cells.

The evaporative heat transfer process, however, is considerably more complex. Water from the electrolyte evaporates from the liquid surface into the surrounding air, absorbing latent heat in the process. The evaporative heat loss is calculated as:

$$P_{\text{evap}} = m_{\text{evap}} \cdot \left(c_{\text{ele}} \cdot T_{\text{ele,surf}} + \Delta H_{\text{evap,wat}}\right) \quad (9)$$

where P_{evap} is the evaporative heat loss of the electrolyte. m_{evap} is the mass evaporation rate of the electrolyte. $T_{\text{ele,surf}}$ is the surface temperature of the electrolyte. $\Delta H_{\text{evap,wat}}$ is the latent heat of vaporization of water.

2) Event-driven Behavior

Event-driven behavior includes the energy input from anode, cathode, electrolyte replenishment insertion and residual anode, cathode copper anode and mud output. That is, the event-driven behavior is characterized by non-differentiable, intermittently periodic, impulse-like changes.

Taking the electrode loading and unloading behavior as an example, the temperature response of the electrolyte differs between the two operation conditions. When electrode loading occurs at a low temperature, the electrolyte temperature initially decreases and then gradually recovers under heating. In contrast, electrode unloading does not cause any noticeable temperature change, as shown in fig. 3.

The magnitude of these variations is determined by the internal energy difference between the materials and the electrolyte. This difference is calculated using specific heat capacity, which quantifies the thermal impact of event-driven input or output processes on the electrolyte temperature.

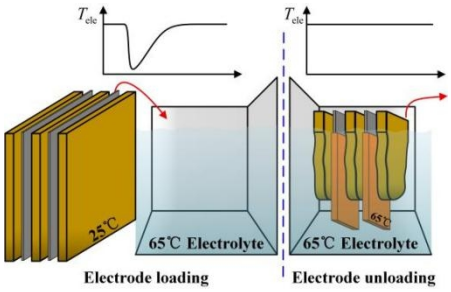

Figure 3. The temperature changes caused by the replacement of the plates.

The calculation method is as follows:

$$E_i \vee \delta_i = c_i \cdot m_i \cdot (T_i - T_{\text{ele}}) \quad (10)$$

where $E_i \vee \delta_i$ is the internal energy of the plates, anode mud or fluid replenishment. c_i is the specific heat capacity corresponding to the above-mentioned material, which can be determined by the proportion of components. m_i and T_i are the mass and temperature of the above-mentioned material, respectively . T_{ele} is the temperature of the electrolyte.

Although the removal of spent anodes and cathode copper reduces the internal energy of the electrolytic system, the temperatures of the electrodes are essentially equal to that of the electrolyte, and the energy and material outputs occur simultaneously. Therefore, this process does not decrease the cell temperature, and thus $\delta_{\text{cath}} = \delta_{\text{ano}} = 0$. Anode mud is generally removed only during cell cleaning. If the electrolytic cell remains uncleaned during the calculation period, the thermal energy associated with anode mud removal can be considered negligible $\delta_{\text{mud}} = 0$.

3) Output of the Digital Model

In practical applications, the digital system is required to provide data such as the cell temperature, cell voltage, and copper production to support monitoring of operating conditions and safety during DR. The corresponding calculations for these three variables are given as follows:

$$T_{\text{ele}} = T_{\text{ele}}^{\text{initial}} + \Delta\Theta_{\text{ele,t}}/c_{ele} \cdot m_{ele} \quad (11)$$

$$U_{\text{ele}} = I \cdot (R_{\text{ele}} + R_{\text{cath}} + \eta_{\text{and}} + \eta_{\text{cath}}) \quad (12)$$

$$m_{\text{cop}} = I \cdot 1.186 \cdot \eta_{\text{ele}} \cdot t \quad (13)$$

where $T_{\text{ele}}^{\text{initial}}$ is the electrolyte temperature. $\Delta\Theta_{\text{ele,t}}$ is the change in internal energy calculated by (1), and m_{ele} is the electrolyte mass at time. U_{ele} denotes the cell voltage, while R_{ele} and R_{cath} are the electrical resistances of the electrolyte and the electrode plates, respectively. m_{cop} is the cathode copper production, 1.186 is the electrochemical equivalent of copper. η_{ele} and t denote the copper production efficiency of the electrolysis cell and the operating time, respectively.

C. Physical Model

The physical model corresponding to the digital model is a scaled-down copper electrolytic cell. Unlike conventional laboratory setups, it is designed to replicate industrial-scale dynamic behavior under controllable conditions. To ensure accurate reproduction of the electrothermal characteristics of an industrial cell, two similarity conditions must be satisfied:

(i) Current density similarity, which guarantees consistent electrochemical kinetics and overpotential behavior;

(ii) Volumetric heat generation rate similarity, which governs the temperature evolution and, in turn, influences the electrochemical reaction rate.

$$I = I_{\text{dens}} A_{\text{cath}} = J_p s^2 A_p \tag{14}$$

$$I_{\text{dens}}^2 / \sigma_{\text{ele}} \approx J_{\text{p}}^2 / \sigma_{\text{p}} \tag{15}$$

where J_{p} is the current density of the industrial cell. s denotes the characteristic length ratio between the industrial and model cells. A_{p} is cathode plate area of the industrial cell. σ_{p} represents the electrolyte conductivities of the industrial cells.

D. Bridging Between Digital-Physical Models

During digital-physical hybrid simulation, the digital system executes DR commands and scales parameters per physical similarity. A Modbus-TCP-based communication layer integrates all device units on a common bus for real-time acquisition of temperature, cell voltage, and pump frequency. These parameters serve as control signals via the Modbus server. When deviations between simulated and measured values exceed the threshold, a correction coefficient adjusts the data and feeds it back to the digital model, achieving closed-loop synchronization, expressed as:

$$\boldsymbol{u}_{\text{act}} = \boldsymbol{S}\boldsymbol{u}_{\text{sim}} \tag{16}$$

$$\boldsymbol{u}_{\text{sim}}^{\text{new}} = \boldsymbol{u}_{\text{sim}}^{\text{old}} + \boldsymbol{K}_{\text{c}}(\hat{\mathbf{x}}_{\text{k|k}} - \boldsymbol{x}_{\text{sim,k}}) \tag{17}$$

where u_{act} represents the actual operating parameters applied by the physical execution layer. $\boldsymbol{S}$ is the scaling matrix, used to map the simulation parameters to the laboratory scale. $\boldsymbol{u}_{\text{sim}}$ denotes the output parameters of the simulation system. $\boldsymbol{K}_{\text{c}}$ is the correction gain matrix, which adjusts the feedback intensity by amplifying or attenuating the error. $\hat{\mathbf{x}}_{\text{k|k}}$ is the measured output of the physical system. $\boldsymbol{x}_{\text{sim,k}}$ is the predicted output of the digital model.

The data interaction between the digital and physical systems are detailed in Fig. 4. During DR, the response is primarily achieved by adjusting the heating power of the electrolysis cell (i.e., cell temperature), the cell current (with a corresponding change in cell voltage), and the pump frequency.

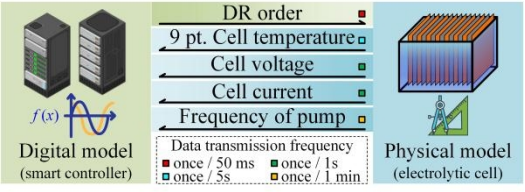

Figure 4. Data transmission between the digital and physical systems.

III. Case Study

A. The Structure of the Physical Model

The total volume of the electrolyte is 75 L, and the cell consists of five anodes and four cathodes. Each cathode plate measures 280 × 230 mm. The electrolyte circulation is driven by an acid-resistant variable-frequency pump with a rated power of 45 W, operating in a bottom-inlet, top-outlet configuration. A heating chamber equipped with a 3 kW acid-resistant heating rod is used to maintain the electrolyte temperature. The structural configuration of the electrolytic cell is illustrated in Fig. 5.

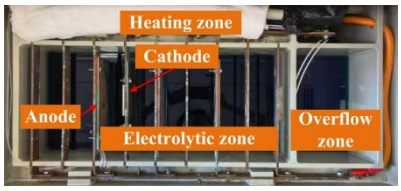

Figure 5. Structure of the copper electrolytic cell.

B. Construction of a Digital-Physical Hybrid System

During coordinated operation, the digital subsystem runs on a smart terminal, while the physical electrolytic cell is activated. Selected parameters from the physical system are transmitted via signal wires to support digital subsystem operation. Meanwhile, the digital system issues control commands and monitors the physical subsystem in real time. The overall digital-physical hybrid platform bridging both systems is shown in Fig. 6 (a).

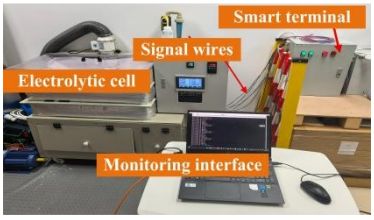

(a) Connectivity of hybrid system

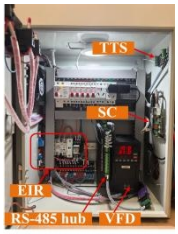

(b) Consists of smart terminal

Figure 6. Digital-physical hybrid system connectivity.

The smart terminal consists of the following key components and their respective functions. The smart controller (SC) executes digital system codes, manages the physical system, and enables information-level interaction between the digital and physical systems. The terminal temperature sensor (TTS) monitors cabinet temperature and controls the cooling fan to prevent SC overheating. The variable-frequency drive (VFD) regulates the circulation pump speed and flow rate. The electrical isolation and relay (EIR) module controls the electrolyte temperature and heating system. The RS-485 Hub aggregates communication from multiple measurement points-cell temperature, cell voltage, cell current, circulation flow rate, and cabinet temperature and transmits data between the SC and subsystem devices, as shown in Fig. 6 (b).

C. Verification of Digital Model

Although the physical system assists the digital system in real-time state correction, the latter must still maintain high

computational accuracy during short-term prediction to prevent significant deviations. During model validation, the accuracy of the calculated cell voltage at different electrolyte temperatures was assessed. Cell voltage was chosen as the key validation metric due to its strong correlation with temperature and its role as a major energy consumption indicator in electrolytic production. The electrolytic cell was operated from 45 °C to 70 °C, with a 12 W circulation pump running continuously for about 1.23 h of heating. During this period, the digital model operated independently without external correction. Comparison between calculated and measured voltages yielded the variation and error distribution of cell voltage, as shown in Fig. 7.

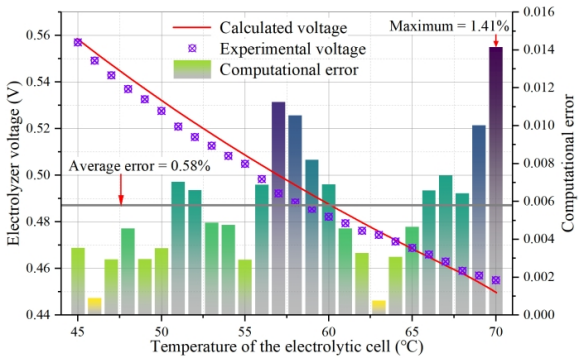

Figure 7. Cell voltage calculation performance and error distribution.

By comparing the experimental and simulated data, the average error of the cell voltage calculation was approximately 0.58%, with the maximum error of 1.41% occurring at 70 °C. Under normal operating conditions (around 65 °C), the calculation exhibited high accuracy and stable performance.

D. Verification of Digital-Physical Model Hybrid Operation

During the operation of the digital-physical hybrid simulation, continuous data exchange was maintained between the physical and digital models. To verify the feasibility and accuracy of the digital-physical hybrid simulation system for investigating the participation of copper electrolysis cells in DR, the experiment was conducted over a duration of 2.5 h, including 0.5 h of DR (reducing the load by 35%). Upon completion, experimental data from the digital model and the measured mass of cathode copper from the physical model were compared, as shown in Fig. 8.

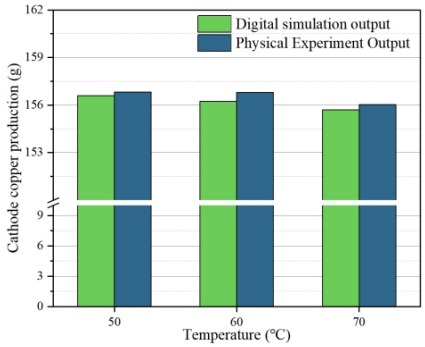

Figure 8. Digital-physical hybrid simulation performance.

Validation based on cathode copper production indicates that the digital model slightly underestimates the yield compared to the physical model. The maximum discrepancy occurs at 60 °C, while the overall error across all tested temperatures remains below 1.3%. These results demonstrate that the digital model performs reliably in predicting production outcomes.

IV. CONCLUSION

Based on the digital-physical hybrid simulation study of the copper electrorefining process, the following conclusions are drawn:

1) The model accurately captures the key characteristics of the electrolysis process, with the cell voltage calculation error below 0.6% and the predicted cathode copper yield error not exceeding 1.3%.

2) The constructed digital–physical hybrid platform enables real-time data exchange and model correction, providing reliable predictions of process parameters under variable operating conditions.

3) The hybrid simulation platform effectively enhances the precision of industrial energy management. Practical value is demonstrated in investigating the dynamic characteristics of industrial loads during DR via coordinated digital-physical operation.

ACKNOWLEDGMENT

The authors would like to express their sincere gratitude to Yunnan Copper Co., Ltd. for the valuable support provided during the course of this research.

REFERENCES

[1] S. Deetman, S. Pauliuk, D. P. van Vuuren, E. van der Voet, and A. Tukker, "Scenarios for Demand Growth of Metals in Electricity Generation Technologies, Cars, and Electronic Appliances," *Environmental Science & Technology*, vol. 52, no.8, pp. 4950-4959, Mar. 2018.

[2] IEA, "The Role of Critical Minerals in Clean Energy Transitions," *Rep ort, International Energy Agency*, 2021, https://www.iea.org/reports/the -role-of-critical-mineralsin-clean-energy-transitions.

[3] F. T. C. Roben, D. Liu, M. A. Reuter, M. Dahmen, and A. Bardow, "Th e demand responsepotential in copper production," *Journal of Cleaner Production*, vol. 362, pp. 132221, Aug. 2022.

[4] ICA, "Copper Environmental Profile," *Report, International Copper As sociation*, https://internationalcopper.org/wp-content/uploads/2021/08/I CA-EnvironmentalProfileHESD-201803-FINAL-LOWRES-1.pdf.

[5] H. Khayatzadeh and K. Tahmasebi, "Optimizing Electrolyte Conditions for theElimination of Nodules in Copper Electrorefining Process," *JO M*, vol. 76, no. 1, pp. 452-463, Nov. 2023,

[6] J. M. Werner, w. Zeng, M. L. Free, Z. Zhang, and J. Cho, "Editors'Choi ce-Modeling andValidation of Local Electrowinning Electrode Current Density Using Two Phase Flow andNernst-Planck Equations," *Journal of The Electrochemical Society*, vol. 165, no. 5, pp.190-207, Mar. 2018.

[7] M. Moats and J. Dolinar,"The effect of electrolyte additives on cathode surface quality during copper electrodeposition," *J. Appl. Electrochem.*, vol. 41, no. 5, pp. 371-378, May 2011.

[8] S. Kawai and T. Miyazawa, "CFD modelling and simulation of industri al-scale copperelectrorefining process," *Minerals Engineering*, vol. 63, pp. 81-90, Aug. 2014.

[9] T. Kalliomäki et al., "Industrial validation of conductivity and viscosit y models for copperelectrolysis processes," *Minerals Engineering*, vol. 171, pp.107069, Sep. 2021.